International Institute for Applied Systems Analysis
IIASA www.iiasa.ac.at

Timing of the emergence of new successful viral strains in seasonal influenza

Omori, R. and Sasaki, A.

IIASA Interim Report
2013

International Institute for
Applied Systems Analysis
Schlossplatz 1
A-2361 Laxenburg, Austria

Tel: +43 2236 807 342
Fax: +43 2236 71313
E-mail: publications@iiasa.ac.at
Web: www.iiasa.ac.at

Interim Report **IR-13-056**

Timing of the emergence of new successful viral strains in seasonal influenza

Ryosuke Omori
Akira Sasaki (sasaki@iiasa.ac.at)

Approved by

Ulf Dieckmann
Director, Evolution and Ecology Program

June 2015

Timing of the emergence of new successful viral strains in seasonal influenza

Ryosuke Omori[1,*] and Akira Sasaki[2,3,4]

[1] School of Public Health, The University of Hong Kong, Level 6, Core F, Cyberport 3, 100 Cyberport Road, Hong Kong;

[2]Department of Evolutionary Studies of Biosystems (Sokendai-Hayama), The Graduate University for Advanced Studies (Sokendai), Hayama, Kanagawa 240-0193, Japan;

[3]Evolution and Ecology Program, International Institute for Applied Systems Analysis, A-2361 Laxenburg, Austria;

[4]PRESTO, Japan Science and Technology Agency, 4-1-8 Honcho Kawaguchi, Saitama, Japan

[*]To whom correspondence should be addressed. E-mail: r.omori12@gmail.com

Abstract

High evolvability of influenza virus and the complex nature of its antagonistic interaction with the host immune system make it difficult to predict which strain of virus will become epidemic next and when it will emerge. To investigate the most likely time at which a new successful strain emerges every year in seasonal influenza, we use an individual-based model that takes into account the seasonality in transmission rate and host cross-immunity against a current viral strain due to previous infections with other strains. Our model deals with antigenic evolution of influenza virus that originated by point mutations at the antigen determining sites and is driven by host immune response. Under the range of parameters by which influenza virus shows a "trunk" shape in its phylogenetic tree, as is typical in influenza A virus evolution, we find that most successful mutant strains emerge in an early part of the epidemic season, and that the time when the number of infected hosts reaches a maximum tends to be more than one season after viral emergence. This carryover of the epidemic peak timing implies that we can detect the strain that will become dominant in the epidemic in the following year.

1. Introduction

Influenza viruses rapidly change their antigenicity (antigenic drift), which makes vaccination strategy against them difficult. Forecasting the evolutionary trajectory of influenza antigenicity is therefore important for prevention of an epidemic. The evolution of influenza virus is driven by selection due to changes in the host herd immunity, as well as random factors such as mutations, demographic stochasticity due to finiteness of infected hosts, and environmental fluctuation. The combined effect of these factors should mold the direction of the evolutionary trajectory. A new viral strain must face not only the immune response directly mounted against it, but also partial cross-immunity due to previous infection with related strains. In addition to the specific immune responses, a novel infecting strain must face temporal nonspecific immunity raised by infection with strains with arbitrary antigenicity (Ferguson et al. 2003). These immune-driven processes should play a key role in the evolution of influenza virus. The immune response due to earlier infection can suppress later emergence of an epidemic outbreak with other strains, which could drive the later strains to extinction. This 'mass extinction' of later strains that would establish themselves if originated earlier can make the phylogenetic tree of influenza virus slender (Andreasen et al., 1997, Ferguson et al., 2003, Koelle et al., 2006, Andreasen and Sasaki, 2006, Omori et al., 2010).

The genetic distance is correlated with the antigenic distance (Smith et al. 2004), and the strength of host herd immunity against a new strain of influenza virus is determined by how far it is genetically or antigenically distant from the strains that the host population has experienced in the past. Mathematical models that explicitly take into account the phylogenetic relationship between strains are therefore necessary to understand the evolution of influenza virus. In this paper, we study the model describing

the evolution of antigenic sites of virus, in which viruses are allowed to mutate their antigenicity and the antigenic variants are exposed to selection due to host and cross immunity. This is a multi-strain model with cross immunity that describes the coupled dynamics of host herd immunity structure and the epidemiology of co-circulating viral strains. Previous studies based on multi-strain models have revealed which strains may be dominant at equilibrium and how the equilibrium may be destabilized (Gupta et al., 1996, Minayev and Ferguson, 2009, Recker et al., 2007). By using our individual based model for the co-circulation of antigenic strains, we focus on the timing of emergence, epidemic peak timing and epidemic duration of influenza virus strains that will successfully establish themselves in the host population.

2. Model

We consider a host population of a finite size, say 10^5, and track the immune status of each host individual against each virus strain. We designate the immune status of the x-th person against a viral strain n by $H_{x,n}$:

$$H_{x,n} \in \{0,1,2\}, \tag{1}$$

where the state 0, 1 and 2 respectively indicates that the host is susceptible to, currently infected by, and recovered from the viral strain n. We consider the immunity and cross-immunity against a viral strain in terms of the infectivity of the strain. For example, the force of infection Λ_A of strain A, or the rate at which a host is infected by strain A, is defined as

$$\Lambda_A = \beta \sum_{x \mid H_{x,A}=1} \tau_{x,A}, \tag{2}$$

where summation is taken for all the hosts, x, infected by strain A (i.e. with the state

$H_{x,A}=1$). β is the transmission rate of virus, constant over strains, but has seasonal variation within an annual cycle

$$\beta(t)=\beta_0(1+a\cos(2\pi t)), \tag{3}$$

where β_0 is the mean transmission rate, and a the amplitude of seasonal fluctuation of the transmission rate. $\tau_{x,A}$ is the infectivity of strain A reduced by cross-immunity of the *x*-th person,

$$\tau_{x,A}=\min_{B|H_{x,B}=2}(1-\alpha^{d(A,B)}). \tag{4}$$

Here we assume that the closer the antigenic distance $d(A,B)$ between strains A and B, the stronger the degree of immune protection, $\alpha^{d(A,B)}$, by cross immunity, where α is a constant, representing infectivity reduction rate by one mutation, in the range $0<\alpha<1$. The infectivity of a strain A is assumed to be determined by the strongest cross-immunity in all the past infections of *x*-th person. This corresponds to the minimum infectivity of all the viral strains B that have infected the host x in the past.

The antigenic distance (immunological distance) $d(A,B)$ is defined as the number of unmatched sites (hamming distance) between antigenic determining sites of strains A and B. We consider a sequence of antigenic determining sites of length 10, in which each site harbors one of two alleles, 0 and 1. Each site changes its allelic status by mutation with the rate μ.

An infected host recovers at the rate γ. After the recovery, the host achieves temporary nonspecific immunity. Hosts in this class are protected from any strain. Temporary immunity is lost at a constant rate ν. For the sake of simplicity, birth and death rates of a host, denoted by u, are assumed to be the same so that the total

population is kept constant, and newborns are susceptible to all the strains. The mean basic reproductive ratio averaged over a year is expressed by $\bar{R}_0 = \beta_0 / (u+\gamma)$. The initial condition is that the host population is completely susceptible to any strain, except for 10 host individuals infected by a single inoculated strain with the sequence of antigenic determining sites 00…0. Birth and death of hosts, infection and recovery events, and mutations at antigenic sites of influenza virus occur randomly with the rates described above (the model therefore falls into the category of a multi-agent continuous-time Markov chain).

Previous studies have revealed that, to realize a slender phylogenetic tree that characterizes the evolutionary pattern of influenza A virus, the epidemiological parameters must reside in a certain range. In the model of *intra*-host antigenic drift of pathogens, Sasaki and Haraguchi (2000) has shown that an intermediate basic reproductive ratio is necessary for long persistence of viruses by continuously escaping the host immune response. For antigenic drift of pathogens through *inter*-host selection pressure as in the present model, too, small (but being greater than 1) basic reproduction number, as well as sufficiently strong general temporary immunity or suppression of co-infection is necessary for secure long persistence of a slender phylogenetic tree during antigenic drift (Andreasen and Sasaki, 2006, Omori et al., 2010, Koelle et al., 2010, Bedford et al., 2012). Fig. 1a shows a phylogenetic tree observed in our individual based model simulation and Fig. 1b shows the mean antigenic distance between strains co-circulating at each time point:

$$\bar{d}(t) = \frac{\sum_A \sum_{B|B\neq A} [I_A(t) I_B(t) d(A,B)]}{\sum_A \sum_{B|B\neq A} [I_A(t) I_B(t)]}, \qquad (5)$$

where $d(A,B)$ is the antigenic distance between strain A and B, and $I_A(t)$ and $I_B(t)$ is the number of hosts infected by strain A and stain B, respectively, at time t. These results show that the within-year antigenic diversity of viruses is kept low and the phylogenetic tree is kept slender in our model. We are interested in the long-lasting antigenic drift of pathogens as found in influenza viruses; therefore, we restricted our analysis in the range of epidemiological parameters of cross-immunity and general temporary immunity (β, ν, α and a), so that the viruses succeeded in persisting for >1000 years by continuously evading the immune response in the simulation. If co-infection is not suppressed, sufficiently strong general temporal immunity is required (Fig. A1), which agrees with the findings of Andreasen and Sasaki 2006 and Omori et al. 2010. In the case where co-infection is suppressed, the lineage of virus can persist for a long time even if there is no general temporal immunity. Other parameters are kept constant : γ = 25.0 per year by which the infectious period $1/\gamma$ is set about 2 weeks, u = 1/50 by which mean host life time is 50 years, and mutation rate per antigenic site per infection event $\mu = 0.001$. Most simulations are performed with host population size of N=10^5, but the results remained qualitatively similar when N was further increased (up to 10 times larger) as long as $N\beta$ is kept constant to give rise to the same basic reproductive ratio.

3. Results

3.1 Earlier emergence of successful strains than in the seasonal peak in transmission efficiency

We first focus on the emergence times of new strains in a year observed in our

Monte Carlo simulations. The peak time for the generation of new strains is earlier than the time at which the seasonally varying infection rate attained its maximum (Fig. 2 *A*). Here, we define a new strain of virus as one that has at least one mutation at antigenic determining sites from its direct ancestor. We then focus on a subset of new strains that will later succeed in producing further new strains (Fig. 2 *B–D*). We call these strains the second-generation-producing strains. Among a large number of new viral strains generated by mutations in each year, only a small fraction can establish themselves in a host population (compare the vertical axis of Fig. 2 *A* with those of Fig. 2 *B–D*). All the other new strains become extinct without showing any detectable increase in the population. As a result, the shape of the phylogenetic tree becomes nearly linear, as has been shown empirically for influenza A viruses (Buonagurio et al, 1986, Cox and Subbarao, 2000, Fitch et al., 1991, Fitch et al., 1997 Hay et al., 2001). The second-generation-producing strains in our simulations thus correspond to the strains constituting the "trunk" of the cactus-shaped phylogenetic tree of influenza virus.

Let us now consider the emergence time; the time at which the second-generation-producing strains are generated by mutation. The peak times of emergence of the second-generation-producing strains are earlier than those for all the strains (compare Fig. 2 *B* with Fig. 2 *A*). Though we also study the peak times of emergence of the third- and fourth-generation-producing strains, they show no clear differences from that of the second-generation-producing strains (Fig. 2 *B–D*). This means that, although success in producing the second generations crucially depends on the timing of emergence, further success in producing third or further generations is nearly independent of the emergence time of the strain.

Markedly earlier emergence of successful second-generation-producing strains

during the year is shown over a wide range of parameters (Fig. 3). The emergence times in a single epidemic season of the second-generation-producing strains are consistently and considerably earlier than the mean emergence times of all the new strains, including those that become extinct before increasing in the host population (red, blue, green lines in comparison to black lines in Fig. 3).

3.2 Peak emergence time and basic reproductive ratio

Although the successful strains emerge earlier than the other strains consistently over a wide range of parameters, the mean emergence times themselves change with each epidemiological parameter. The increased mean basic reproductive ratio, $\overline{R}_0$, leads to an earlier peak time of emergence of all the new strains (Fig. 3 *A*). This can be simply ascribed to the classical result of epidemiological models (e.g. Anderson and May, 1991) – an earlier peak of outbreak for a larger basic reproductive ratio. It is interesting to note that for a sufficiently large $\overline{R}_0$, the mean emergence time is set back again due to demoted synchronizations of epidemiological outbreaks by different strains (denoted by larger variances in peak emergence times towards larger $\overline{R}_0$ – see Appendix for the theoretical explanation for the demoted synchronization with a larger basic reproductive ratio). Similarly, the decrease in the degree of cross-immunity (decreased α) by a single mutation in antigenic sites leads to an earlier peak of emergence (Fig. 3 *B*). We also observe that a stronger general temporal immunity (i.e. longer mean duration) leads to an earlier peak of emergence (Fig. 3 *C*). There is no clear effect of the amplitude (a) of seasonal fluctuation of transmission rate (Fig. 3 *D*).

3.3 Carryover of epidemic peak to the next year

We next focus on the time for a strain to attain the maximum for the number of

infected hosts after it emerges. Fig. A2 shows that, during the epidemic courses of particular strains, most epidemic peaks are attained around 1 year after their emergence. This means that, in most cases, the strain that causes an epidemic already emerged in the previous epidemic season, suggesting the possibility for specifying the most likely strain that will become dominant in the next year by looking in the current epidemic season. However, if $\bar{R}_0$ is too large, this is no longer the case; thus, there is a high probability of such a prediction failing. If $\bar{R}_0$ is large, many strains attain their epidemic peaks in the same season in which they emerge. This means that, even at the late stage of the epidemic season, it is too early to find the potential dominant strains of the next season if the basic reproductive ratio is large.

The other parameters (α for cross immunity, $1/\nu$ for general immunity and a for the magnitude of seasonal variation) make only a small difference to the fraction of hosts that are infected in the first year in which the strain emerges. However, they make a big difference in the fraction of hosts that are infected in the second year after the strain emerged. The increased infectivity reduction rate α, prolonged duration of temporal immunity $1/\nu$, and decreased amplitude a of seasonality in transmission rate a, all contribute to reduce the number of hosts who were infected in the second year after the strain emerged. Despite these parametric dependencies for the infection timing spectrum after the second year, the mean time of infection is not changed greatly by α, $1/\nu$ or a, because they hardly affect the number of hosts who are infected in first year in which the strain emerges.

4. Discussion

We studied evolutionary dynamics of influenza in a single population with seasonal change of transmission rate. Present study shows two key results, i) the emergence time of successful strains is earlier than the other strains ii) most strains reach epidemic peak more than 1 year later since their emergence time.

The reason why the emergence time of successful strains (second-generation-producing strains) is earlier than the other strains can be explained by the advantage of strains emerging at an early stage of the epidemic season over the other strains (Omori et al., 2010). An earlier-emerging strain in an epidemic season suffers less from cross-immunity or temporal immunity mounted against the other strains. Later-emerging strains, however, are more heavily suppressed by the cross-immunity of hosts infected by antigenically similar strains. General temporary immunity also contributes to the advantage of an earlier strain, in the same way as cross-immunity does. This by no means implies that the strain with the earliest emergence in the season becomes the major strain of the year; the strains emerging too early must face smaller transmission rates (which fluctuate seasonally) than in the peak season. There is therefore an optimum time of emergence in a year for a mutant virus to be successful, which is much earlier than the peak time of the epidemic of wild-type virus, and against which we must be precautious.

We observed most strains reach epidemic peak more than 1 year later since emergence timing (Fig. A2). This carryover of epidemic peak of a strain from the season it emerges to the next or later epidemic seasons could be important for predicting new successful strains. What, then, enables this carryover? To answer this question, we constructed a deterministic model for the epidemics of a single strain in the host population, in which the immune structure changes with time according to the mean

behavior observed in the individual-based model (IBM) simulation. The epidemic peak timing of the model agrees with, or is self-consistent with, the result of the IBM (Fig. A2). Prohibition of co-infection and addition of general temporal immunity both contribute to carry over the epidemic peak timing of the strains that emerge in the early part of the season. In Fig. A2, the median waiting time to epidemic peak of strains from their emergences discontinuously shifts at the emergence time around $t = 0.8$ in a year. This shift in median waiting time is caused by seasonality of transmission rate,--- for the majority of strains that emerged after the time $t = 0.8$ in a year, their epidemic peaks tend to be carried over to the next season. This discontinuous change of waiting time is expected both in our IBM simulations and our simple mean field model described in Appendix A.

We also analyzed the dependence of the epidemic duration of the second-generation-producing strains on the parameters $\overline{R}_0$, α, $1/\nu$ and a. The epidemic duration is defined as the period from the emergence of the first infectious host to the time when the last infectious host recovers. The results in Fig. A3 can be summarized as follows: the epidemic duration increases if $\overline{R}_0$ increases, and if α and a decrease. There is, however, no clear effect of general temporal immunity, $1/\nu$, on the epidemic duration.

A larger basic reproductive ratio shortens the epidemic duration in the susceptible–infected–recovered (SIR) model if there were only one strain (i.e. in a standard SIR model) (Fig. A4). In contrast, in the IBM model with many co-circulating strains, the increase in the mean basic reproductive ratio, $\overline{R}_0$, leads to an increase in the epidemic duration of the second-generation-producing strains (Fig. A3a). To understand

this discrepancy in the dependence of epidemic duration on $\overline{R}_0$, we focus on the role of competition between co-circulating strains for their hosts. For a larger number of co-circulating strains, we expect more intense competition between them, and hence we expect a smaller peak of epidemic and prolonged epidemic duration by each strain. This is supported by the IBM model. We find that the total number of hosts infected in a season increases with $\overline{R}_0$ (Fig. A5 *A*), but that the mean number of hosts infected by each strain decreases with $\overline{R}_0$ (Fig. A5 *C*). This is because the "denominator", the number of emerged strains per season, increases further than the "numerator", the total number of infected hosts, with $\overline{R}_0$ (compare Fig. A5 *A* with A3 *B*). Similarly, a longer epidemic duration with a smaller α (Fig. A3 *B*) suggests that more efficient cross-immunity by a single mutation (i.e. decreased α) leads to more intense competition between co-circulating strains.

The reason why a greater fluctuation in transmission rate (by increased *a*) shortens epidemic duration of the second-generation-producing strains (Fig. A3 *D*) can also be explained by more intense competition between co-circulating strains. Indeed, the denominator of mean number of hosts infected by a particular strain (i.e. number of strains that emerged in a season) increases further than the numerator (i.e. total number of infected hosts) with increasing *a* (Fig. A6 *A* and *B*). (15) has revealed that epidemics of influenza A in high latitude regions have stronger seasonality than those in low latitude regions, therefore it is suggested that epidemics of each influenza strain in low latitude region should persist longer.

General temporal immunity shows no clear effect on epidemic duration (Fig. A3 *C*). This is consistent with the fact that there is no clear difference in the mean number

of hosts infected by the second-generation-producing strains that emerge in a season for varying $1/\nu$ (Fig. A7 *C*). A greater general temporal immunity (i.e. longer duration) decreases to the same extent both the total epidemic size and the number of strains emerging per year (Fig. A7 *A* and *B*).

We studied the evolutionary dynamics of seasonal flu by assuming seasonal change in the transmission rate, without introducing meta-population structure and the processes of local extinction and reinvasion of viruses. Several studies argue that evolutionary dynamics of influenza is affected by the migration of influenza virus from other areas (Bahl et al. 2011, Bedford et al. 2010, Bedford et al. 2012, Russell et al. 2008). In temperate region where strong seasonality in epidemic is observed, the morbidity during non-epidemic season is indeed very low (Rambaut et al. 2008). However, considering host heterogeneity and environmental heterogeneity within a local population, perfect extinction of the whole strains may not always occur even in non-epidemic season. Our results clearly show that even without meta-population structure or geographical heterogeneity, the viruses can securely be maintained and perform rapid and consecutive antigenic evolution. Introducing geographical structure and migration in analyzing viral evolution is definitely quite important, but is out of scope of the present study. Though our study focuses on the evolutionary dynamics at the local area level, we have revealed a number of new findings on the timing of successful emergence and peak epidemic of strains. It is also worth noting that annual cycles of epidemic with nonzero morbidity in non-epidemic season are observed in tropical and subtropical regions (Blair et al. 2009).

The key result of our study is that the strains that will produce new strains tend to emerge at an early stage in the epidemic season, and reach the maximum number of

infected hosts in the next season. This result agrees with that of Omori et al. (2010). Omori et al. (2010) reached the same conclusion for early emergence a new strain that will succeed in establishing itself by analyzing whether or not a new branch can occur on a linear trunk structure of the viral phylogeny of virus. In the present paper, we relaxed these restrictive simplifying assumptions and allowed viruses to have arbitrary phylogenetic relationship and extended their results. Predicting a strain that will become dominant in the next year is usually difficult, but our study suggests that the strains that have already emerged by the time of peak epidemic have a high probability of becoming the dominant strains in the next year. Our main conclusion that epidemic of successful viral strains are likely to be carried over to the next year of their emergence (Figure #) suggest that effort must be focused on the survey of co-circulating strains in the last year that had not yet become dominant and survived till the end of epidemic season.

Acknowledgments

This work was supported in part by the Center for the Promotion of Integrated Sciences (CPIS) of Sokendai, and by the Research Fellowship of Japan Society for the Promotion of Science.

References

Anderson, R. M. & May, R. M. (1991) Infectious Diseases of Humans: Dynamics and Control. Oxford Univ. Press. Oxford.

Andreasen, V., Lin, J. & Levin, S. (1997). The dynamics of cocirculating influenza strains conferring partial cross-immunity. *J. Math. Biol*. 35: 825–842.

Andreasen, V. & Sasaki, A. (2006). Shaping the phylogenetic tree of influenza by cross-immunity. *Theor. Popul. Biol*. 70: 164-173.

Bahl, J., Nelson, M. I., Chan, KH et al. *(2011).* Temporally structured metapopulation dynamics and persistence of influenza A H3N2 virus in humans. *Proc Natl Acad Sci USA* 108: 19359–19364.

Bedford, T., Cobey, S., Beerli, P. et al. (2010). Global migration dynamics underlie evolution and persistence of human inuenza A (H3N2). *PLoS Pathog* 6: e1000918.

Bedford, T., Rambaut, A., Pascual, M. (2012). Canalization of the evolutionary trajectory of the human influenza virus. BMC Biol. 10:38

Blair, P.J., Wierzba, T.F., Touch, S et al. (2009). Influenza epidemiology and characterization of influenza viruses in patients seeking treatment for acute fever in Cambodia. *Epidemiol. Infect.* 138:199–209.

Buonagurio, D., Nakada, S., Parvin, J. et al. (1986) Evolution of human influenza A virus over 50 years: rapid, uniform rate of change in NS gene. *Science* 232: 980–982.

Cox, N.J. & Subbarao, K. (2000) Global epidemiology of influenza: past and present, *Annu. Rev. Med*. 51: 407–421.

Ferguson, N.M., Galvani, A.P. & Bush, R.M. (2003). Ecological and immunological determinants of influenza evolution. *Nature* 422: 423–428.

Fitch, W.M., Leiter, J.M.E., Li, X. et al. (1991) Positive Darwinian evolution in human influenza A viruses, *Proc. Natl. Acad. Sci. USA* 88: 4270–4274.

Fitch, W.M., Bush, R.M., Bender, C.A. et al. (1997) Long term trends in the evolution of H(3) HA1 human influenza type A, *Proc. Natl. Acad. Sci. USA* 94: 7712–7718.

Gupta, S., Maiden, M.C.J, Feavers, I.M. et al. (1996) The maintenance of strain structure in populations of recombining infectious agents. *Nat. Med*. 2: 437–442.

Hay, A., Gregory, V., Douglas A. et al. (2001) The evolution of human influenza viruses. *Phil. Trans. R. Soc. Lond. B* 356: 1861–1870.

Koelle, K., Cobey, S., Grenfell, B. et al. (2006). Epochal evolution shapes the phylodynamics of interpandemic influenza A(H3N2) in humans. *Science* 314: 1898–1903.

Minayev, P. & Ferguson, N. (2009) Improving the realism of deterministic multi-strain models: implications for modelling influenza A. *Interface* 6: 509–518

Omori, R., Adams, B. & Sasaki, A. (2010) Coexistence conditions for strains of influenza with immune cross-reaction. *J. Theor. Biol*. 262: 48-57

Recker, M., Pybus, O.G., Nee, S. et al. (2007) The generation of influenza outbreaks by a network of host immune responses against a limited set of antigenic types. *Proc. Natl Acad. Sci. USA* 104: 7711-7716

Rambaut, A., Pybus, O. G., Nelson, M. I. et al. (2008) The genomic and epidemiological dynamics of human influenza A virus. *Nature* 453: 615-619

Russell, C. A., Jones, T. C., Barr, I. G. et al. (2008) The Global Circulation of Seasonal Influenza A (H3N2) Viruses. *Science* 320: 340-346

Sasaki, A. & Haraguchi, Y. (2000) Antigenic drift of viruses within a host: A finite site model with demographic stochasticity. *Journal of Molecular Evolution* 51: 245-255

Smith, D. J., Lapedes, A. S., de Jong, J. C. et al. (2004) Mapping the Antigenic and Genetic Evolution of Influenza Virus. *Science* 305: 371-376

Figure legends

Fig. 1. (a) Phylogenetic tree is produced with a 100 year simulation result of our model. Strains that the number of infected hosts are smaller than 500 don't appear in phylogenetic tree. (b) Time evolution of weighted mean antigenic distance between emerged stains. For both (a) and (b), simulation settings are same; $\bar{R}_0 = 2$, $\alpha = 0.2$, $1/\nu = 7/365$ (7 days), $a = 0.6$, $1/u = 50$ (years), and $\mu = 0.001$ (per infection).

Fig. 2. Distribution of emergence times of new strains observed in a 1000-year simulation run of the IBM model. (*A*) The solid line indicates the distribution of the emergence timing of new strains that emerge by mutation in each year, with the moving averaged of 1/10 year window. The dashed line indicates the seasonally varying transmission rate. (*B*–*D*) The conditional distributions for the timing of the emergence of strains that succeeded to produce second (*B*), third (*C*), and fourth (*D*) generations. The parameters are set as $\bar{R}_0 = 2$, $\alpha = 0.2$, $1/\nu = 7/365$ (7 days), $a = 0.6$, $1/u = 50$ (years), and $\mu = 0.001$ (per infection).

Fig. 3. The peak emergence times of all the new strains, and the subset of successful (second-, third- and fourth-generation-producing) strains as functions of epidemiological parameters. In each panel, the black line shows the peak emergence time (relative to a year – see the scale of the horizontal axis of Fig. 1) of all the new strains (antigenicity mutants); blue, red and green lines, that of the second-, third- and fourth-generation-producing strains. The epidemiological parameters varied along the horizontal axis of each panel are: (*A*) the mean basic reproductive ratio averaged over a year, $\bar{R}_0 = \beta_0/(u+\gamma)$; (*B*) the infectivity reduction α by the cross immunity mounted

by a single-step distant strain; (*C*) the mean duration of temporal immunity, $1/\nu$; and (*D*) the amplitude of seasonal fluctuation of transmission rate, a. Each point represents the mean value of 10,000 times boot-strap resampling of the simulation results over 1000 years, and the error bars denote their standard deviations. Apart from the parameter values varied in the horizontal axis, the other parameters are set to $\bar{R}_0 = 2$, $\alpha = 0.2$, $1/\nu = 7/365$ (7 days), $a = 0.6$, $u = 1/50$ and $\mu = 0.001$.

Fig. 4. Relationship between the time of the emergence of a strain in a year (horizontal axis) and the waiting time until the number of infected hosts attains its peak since it emerged (vertical axis, in units of year). Note that the transmission was maximum at $t = 0$ or $t = 1$, and minimum at $t = 1/2$. The vertical axis greater than 1 indicates that the epidemic peak was carried over to the next year from the year of emergence. Red points indicate the median waiting time observed in a 1000-year simulation of the IBM model, until a second-generation-producing strain attained its peak epidemic size. Blue points are the result for "mean-field" single strain model described in Appendix, when there is co-infection but no general temporal immunity. Green points are the result for the same mean-field single strain model but there was general temporal immunity but no co-infection. The parameters are $\bar{R}_0 = 2$, $\alpha = 0.2$, $1/\nu = 7/365$ (years, or 7 days), $a = 0.6$, $1/u = 50$ (years) and $\mu = 0.001$.

Fig. A1. Persistence condition of virus in the IBM model when there is co-infection and general temporal immunity. We count the frequency of simulation runs in which the lineage of virus survived for >70 years (over a generation time of the host) in 20

simulation runs of the IBM. In the region marked as "Persistence", the virus survived for >70 years in all 20 simulation runs, whereas in the region marked as "Extinction", the virus became extinct within 70 years in all 20 simulation runs. The parameters except $\bar{R}_0$ and $1/\nu$ were set as $\alpha = 0.2$, $a = 0.6$, $u = 1/50$ and $\mu = 0.001$.

Fig. A2. Cumulative distribution for the timing of infections of all the strains that emerged in a 1000-year simulation of the IBM model. The vertical axis denotes the cumulative distribution for the timing of infection, i.e., the number of hosts infected by a strain by time t, divided by the final epidemic size of that strain. (*A*) The distribution for varying mean basic reproductive rate over a year, $\bar{R}_0$, from 2 to 4; (*B*) that for varying infectivity reduction rate by cross-immunity, α, from 0.1 to 0.3; (*C*) that for varying mean duration of temporal immunity, $1/\nu$, from 2 to 36 days; and (*D*) that for varying amplitude of seasonal fluctuation of transmission rate, a, from 0.3 to 0.6. The basic parameters are set as $\bar{R}_0 = 2$ (*B*–*D*), $\alpha = 0.2$ (*A*, *C* and *D*), $1/\nu = 7/365$ (7 days; *A*, *B* and *D*), $a = 0.6$ (*A*–*C*), $1/u = 50$ (years), and $\mu = 0.001$ (per infection).

Fig. A3. Epidemic duration of the second-generation-producing strain in a 1000-year simulation of the IBM model. Each line denotes mean values of the epidemic duration of the second-generation-producing strains and error bar is standard deviation. Apart from the parameter values varied in the horizontal axis, the other parameters are set to $\bar{R}_0 = 2$, $\alpha = 0.2$, $1/\nu = 7/365$ (7 days), $a = 0.6$, $u = 1/50$ and $\mu = 0.001$.

Fig. A4. Dependence of epidemic duration on basic reproductive ratio in a single strain

SIR model. Time course change of the frequencies of *S*, *I* and *R* in a single strain SIR model was $S' = -\beta SI, I' = \beta SI - \gamma I$, and $R' = \gamma I$. Mean duration of infectiousness is constant, $1/\gamma = 14$ (days), and the basic reproductive ratio β/γ is changed by changing β. Initial condition is $I(0) = 0.000001$, $S(0) = 1 - I(0)$, and $R(0) = 0$. The epidemic duration is defined as the duration from the beginning of the simulation to the time when *I* became smaller than the initial value of *I*, *I*(0).

Fig. A5. Relationship between $\bar{R}_0$ and (*A*) the total number of hosts infected with the second-generation-producing strains that emerged in a season; (*B*) the number of second-generation-producing strains that emerged in a season; and (*C*) the mean final epidemic size of each of second-generation-producing strain, i.e., the mean number of hosts infected by each second-generation-producing strain. (*A*-*C*) are generated from a 1000-year simulation in the IBM model. The parameters except $\bar{R}_0$ are set as $\alpha = 0.2$, $1/\nu = 7/365$ (7 days), $a = 0.6$, u = 1/50 and $\mu = 0.001$.

Fig. A6. Relationship between the amplitude, a, of seasonal fluctuation of the transmission rate and (*A*) the total number of hosts infected with the second-generation-producing strains that emerged in a season; (*B*) the number of the second-generation-producing strains that emerged in a season; and (*C*) the mean final epidemic size of each second-generation-producing strain. (*A*–*C*) are generated from a 1000-year simulation in the IBM model in which the parameters except *a* are set as $\bar{R}_0 = 2$, $\alpha = 0.2$, $1/\nu = 7/365$ (7 days), u = 1/50 and $\mu = 0.001$.

Fig. A7. Relationship between mean duration of temporal immunity $1/\nu$ and (a) the total number of hosts infected with second-generation-producing strains that emerged in a season; (*B*) the number of second-generation-producing strains that emerged in a season; and (*C*) the mean number of the hosts infected by each second-generation-producing strain that emerges in a season. (*A*–*C*) are generated from a 1000-year IBM simulation in which the parameters except $1/\nu$ are set as $\overline{R}_0 = 2$, $\alpha = 0.2$, $a = 0.6$, u = 1/50 and $\mu = 0.001$.

Fig. A8. Relationship between the emergence time (horizontal axis) and epidemic peak time (vertical axis) in a year. The emergence time in a year varied from 0 to 0.99 years, with a 0.01 year interval. The initial condition is that there are a few hosts infected ($I(0) = 0.000001$) and the other hosts are susceptible ($S(0) = 1 - I(0)$, $R(0) = 0$). The mean basic reproductive ratio $\overline{R}_0 = \overline{\beta}/\gamma$ is adjusted by changing $\overline{\beta}$. The parameters are set as $a = 0.6$ and $1/\gamma = 14/365$ (14 days).

Appendix

The demoted synchronization of epidemic peak timing with a larger basic reproductive ratio

For analysis of the relationship between synchronization of epidemic peaks and basic reproductive ratio, we use a standard SIR model (S for the fraction of susceptible hosts, I for that of infected hosts, and R for that of recovered hosts) with seasonal fluctuation of transmission rate,

$$\begin{aligned} S' &= -\beta SI, \\ I' &= \beta SI - \gamma I, \\ R' &= \gamma I, \end{aligned} \tag{A1}$$

where $S + I + R = 1$ and $\beta(t) = \beta_0(1 + a\cos(2\pi t))$. See Fig. A8 legends for the parameter values and initial condition. Using this model, we analyze the relationship between the emergence time in a year (i.e. introduction time of a strain into the host population) and epidemic peak timing in a year. If $\overline{R}_0$ is small, the epidemic peak times in a year are limited to a narrow range in a year when the emergence times vary over a year, whereas if $\overline{R}_0$ is large, the epidemic peak times vary over a wider range in a year (Fig. A8 *A*–*C*). This implies that a smaller $\overline{R}_0$ promotes synchronization of epidemic peak timing in a year among co-circulating strains that emerge at different emergence times.

"Mean-field" model

To understand what makes the carry-over of epidemic peak time, we analyze the key behavior of the IBM model (equations 1–4 in the main text) by constructing a simple deterministic model described below. In the IBM model, the relative infectivity

reduction by cross-immunity in the force of infection of a particular strain is determined by the mean susceptibility of host population to this strain (equations 2 and 4 in the main text). In this model, for the sake of simplicity, we assume that the susceptibility to a particular strain is constant during an epidemic of this strain, and equals the mean value observed in IBM simulations averaged over all emerged strains. Therefore, the force of infection to strain A (equation 2 in main text) is rewritten as

$$\Lambda_A = \beta \bar{Q} i_A, \tag{A2}$$

where i_A denotes the frequency of hosts infected with strain A, $\bar{Q}$ the mean susceptibility and $\beta = \beta_0(1 + a\cos(2\pi t))$.

Under these approximations, we consider the epidemic dynamics of a strain "in the mean field", in which the influence of the other cocirculating strains is embedded in the mean host susceptibility. Suppose that co-infection is possible, but there is no general temporal immunity. The dynamics for the population of each immunity status to strain A, the hosts that are susceptible to strain A (s_A), the hosts that are currently infected and infectious with strain A (i_A), and the hosts that are immune to strain A (r_A), is described as

$$\begin{aligned} s_A' &= -\Lambda_A s_A, \\ i_A' &= \Lambda_A s_A - \gamma i_A, \\ r_A' &= \gamma i_A, \end{aligned} \tag{A3}$$

where $s_A + i_A + r_A = 1$ by definition. We use the mean value of the susceptibility to all strains in a 1000-year simulation of the IBM model with the same parameter values as the value of $\bar{Q}$; $\bar{Q} = 0.85$.

Next, we consider the case in which there is general temporal immunity but

no co-infection. The time course of frequency of each immunity status is rewritten, with equation (S2), as follows

$$\begin{aligned} s_A' &= -\Lambda_A(s_A - \hat{i}(t) - \hat{w}(t)), \\ i_A' &= \Lambda_A(s_A - \hat{i}(t) - \hat{w}(t)) - \gamma i_A, \\ r_A' &= \gamma i_A \end{aligned} \tag{A4}$$

where $\hat{w}(t)$ denotes the frequency of hosts that have general temporal immunity, and $\hat{i}(t)$ the frequency of hosts that are currently infected by some other strain. We use the mean frequency of hosts infected by any strain at each time in a year over 1000 years in the IBM model as $\hat{i}(t)$, and the mean frequency of hosts that have general temporal immunity at each time point in a year over 1000 years in the IBM model as $\hat{w}(t)$. For the calculation of $\hat{i}(t)$ and $\hat{w}(t)$ in the IBM model, the parameters are set as $\overline{R}_0 = 2$, $\alpha = 0.2$, $1/\nu = 7/365$ (7 days), $u = 1/50$ and $\mu = 0.001$.

Fig1

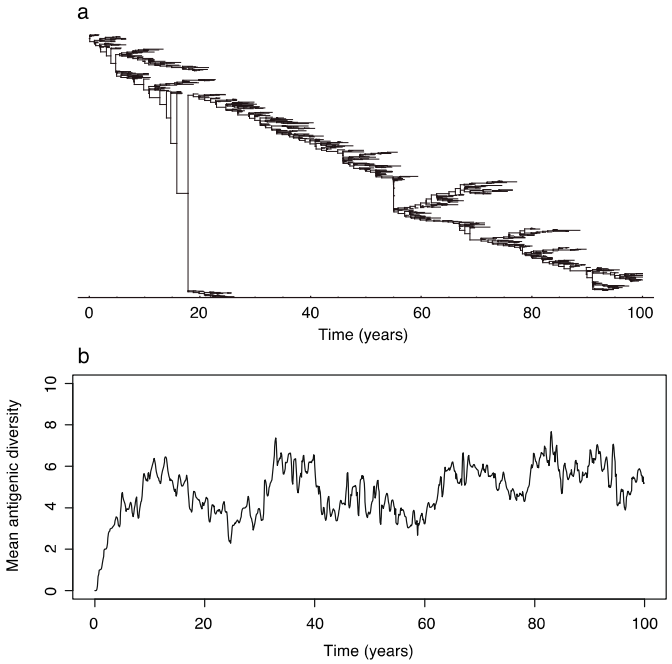
a
0
20
40
60
80
100
Time (years)
b
Mean antigenic diversity
0
2
4
6
8
10
0
20
40
60
80
100
Time (years)

Fig2

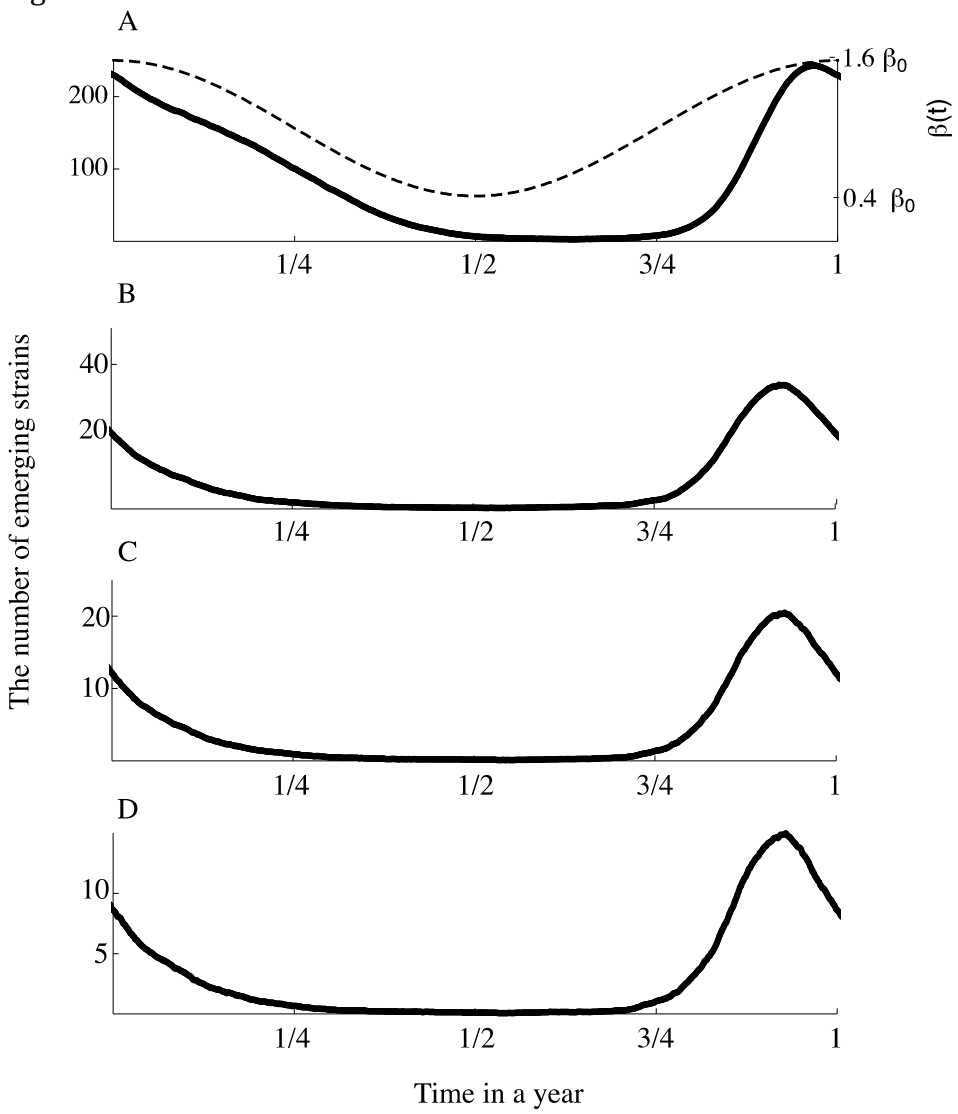
A
200
100
1.6 β0
0.4 β0
β(t)
1/4
1/2
3/4
1
B
40
20
1/4
1/2
3/4
1
C
20
10
1/4
1/2
3/4
1
D
10
5
1/4
1/2
3/4
1
The number of emerging strains
Time in a year

Fig3

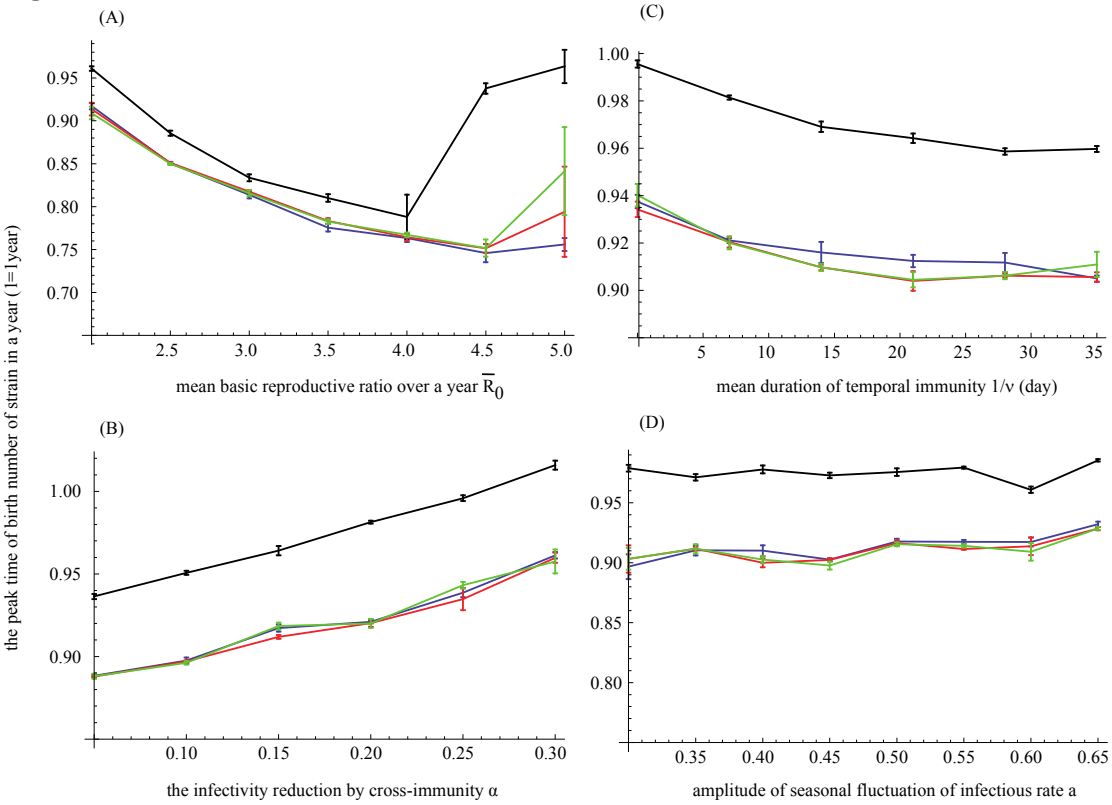
(A)
(C)
(B)
(D)
the peak time of birth number of strain in a year (1=1year)
mean basic reproductive ratio over a year $\overline{R}_0$
mean duration of temporal immunity 1/ν (day)
the infectivity reduction by cross-immunity α
amplitude of seasonal fluctuation of infectious rate a

fig4

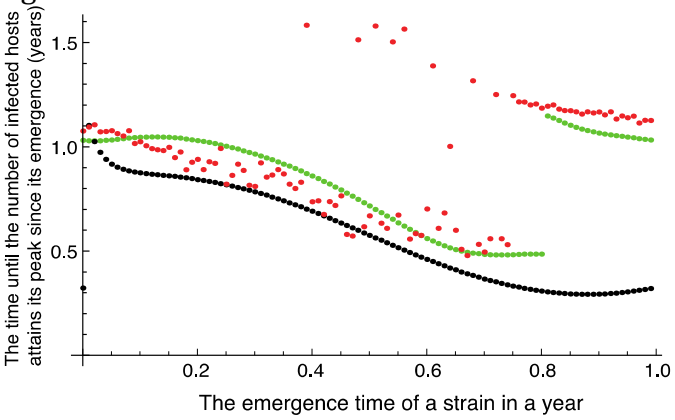
The time until the number of infected hosts attains its peak since its emergence (years)
The emergence time of a strain in a year

FigA1

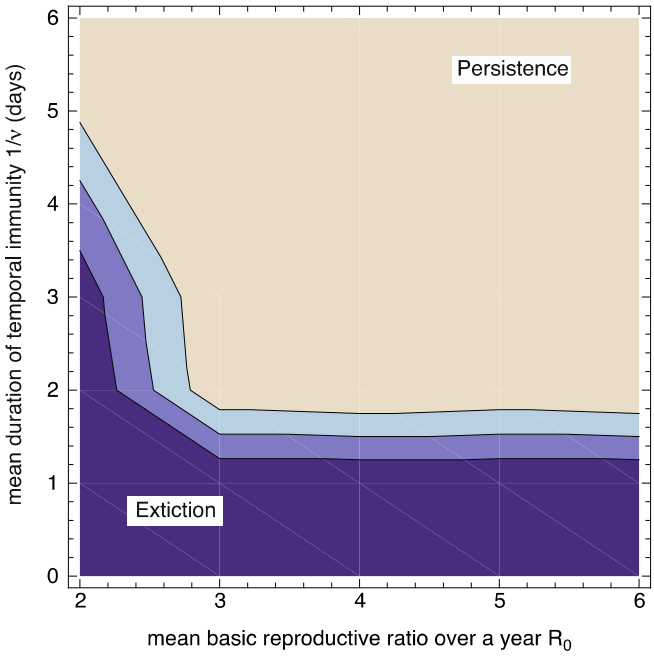
Persistence
Extiction
mean duration of temporal immunity 1/ν (days)
mean basic reproductive ratio over a year R_0

figA2

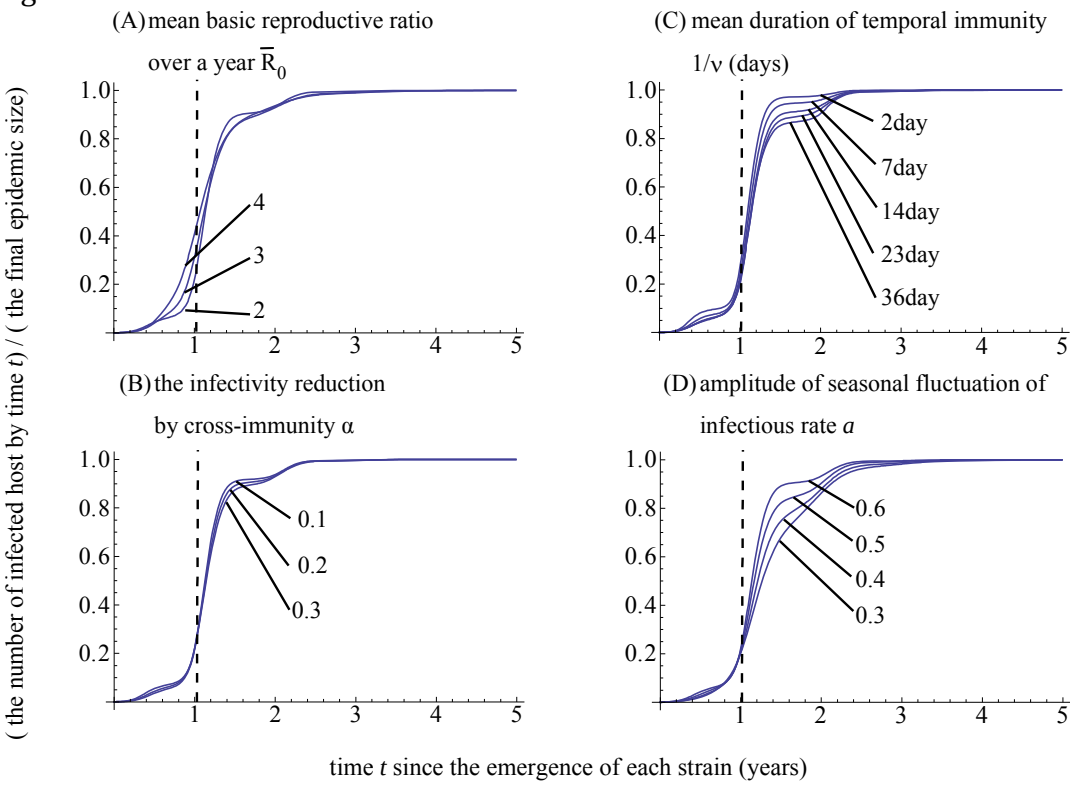
(A) mean basic reproductive ratio over a year $\bar{R}_0$
(C) mean duration of temporal immunity 1/ν (days)
2day
7day
14day
23day
36day
(B) the infectivity reduction by cross-immunity α
0.1
0.2
0.3
(D) amplitude of seasonal fluctuation of infectious rate *a*
0.6
0.5
0.4
0.3
4
3
2
(the number of infected host by time *t*) / (the final epidemic size)
time *t* since the emergence of each strain (years)

figA3

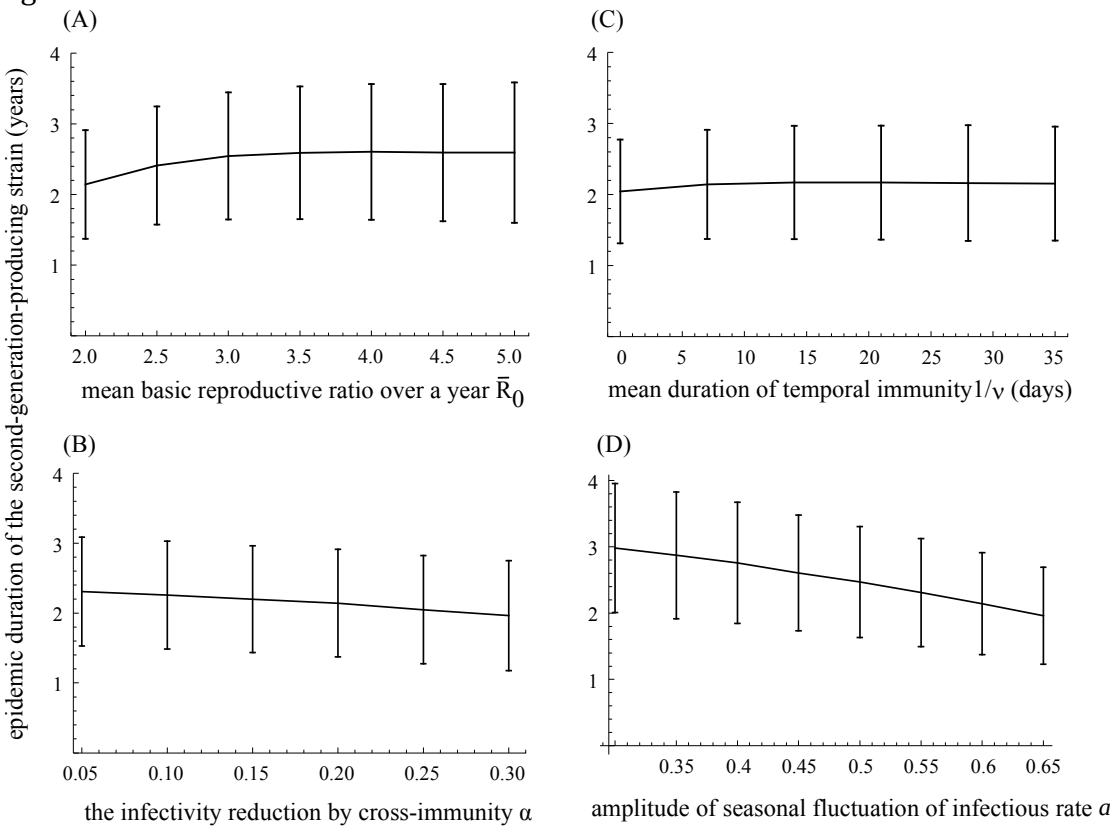
(A)
(C)
(B)
(D)
epidemic duration of the second-generation-producing strain (years)
mean basic reproductive ratio over a year $\bar{R}_0$
mean duration of temporal immunity $1/\nu$ (days)
the infectivity reduction by cross-immunity α
amplitude of seasonal fluctuation of infectious rate *a*

figA4

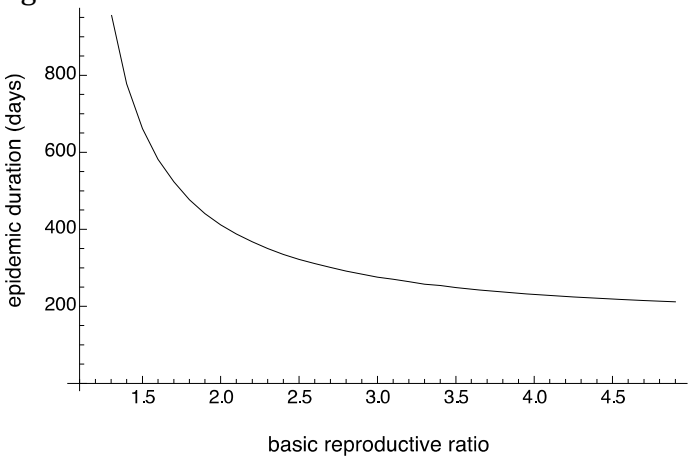
epidemic duration (days)
basic reproductive ratio

figA5

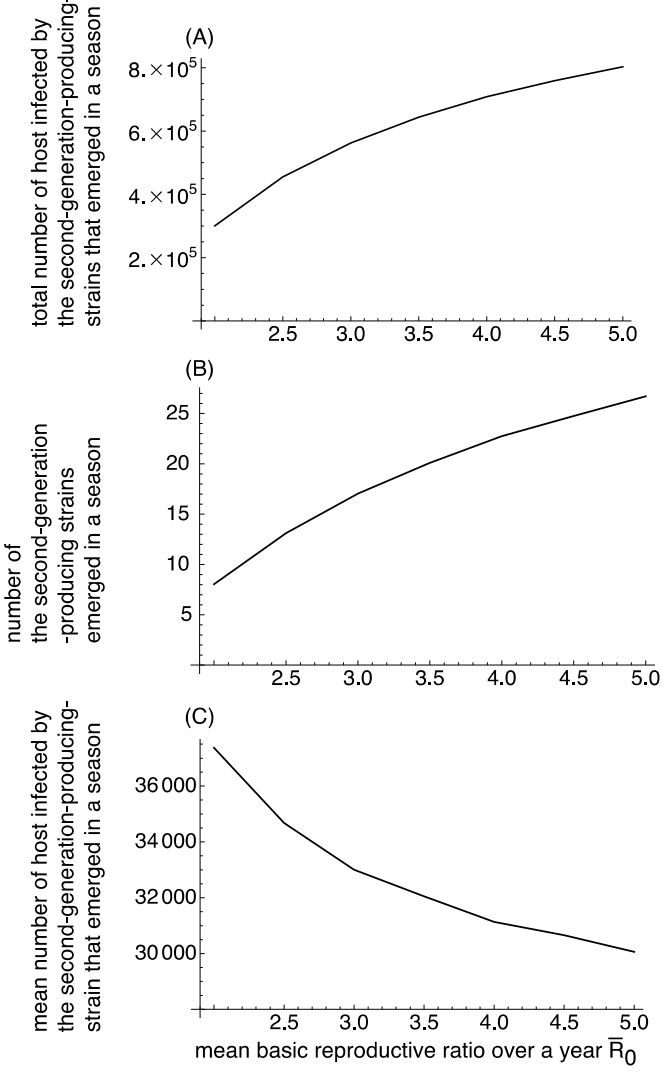
(A)
total number of host infected by the second-generation-producing-strains that emerged in a season
8.×10^5
6.×10^5
4.×10^5
2.×10^5
2.5
3.0
3.5
4.0
4.5
5.0
(B)
number of the second-generation -producing strains emerged in a season
25
20
15
10
5
(C)
mean number of host infected by the second-generation-producing-strain that emerged in a season
36 000
34 000
32 000
30 000
mean basic reproductive ratio over a year $\overline{R}_0$

figA6

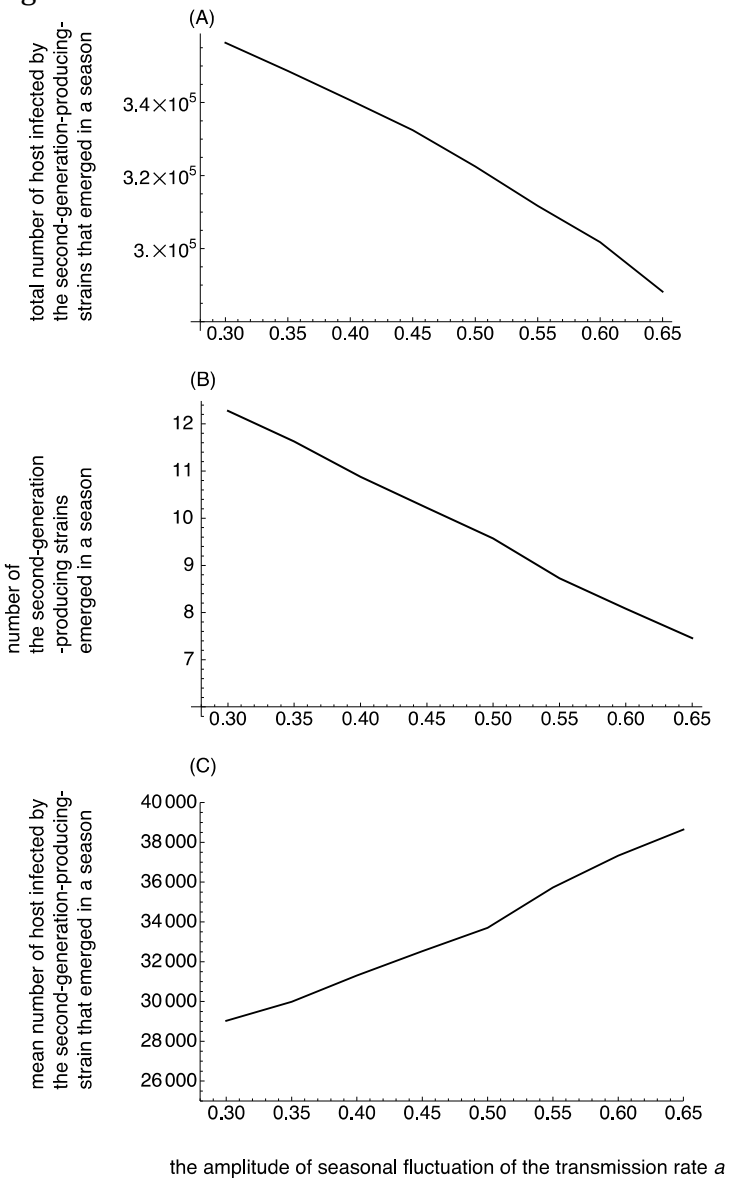
(A)
total number of host infected by the second-generation-producing-strains that emerged in a season
3.4×10^5
3.2×10^5
3.×10^5
0.30 0.35 0.40 0.45 0.50 0.55 0.60 0.65
(B)
number of the second-generation -producing strains emerged in a season
12
11
10
9
8
7
0.30 0.35 0.40 0.45 0.50 0.55 0.60 0.65
(C)
mean number of host infected by the second-generation-producing-strain that emerged in a season
40 000
38 000
36 000
34 000
32 000
30 000
28 000
26 000
0.30 0.35 0.40 0.45 0.50 0.55 0.60 0.65
the amplitude of seasonal fluctuation of the transmission rate a

fig A7

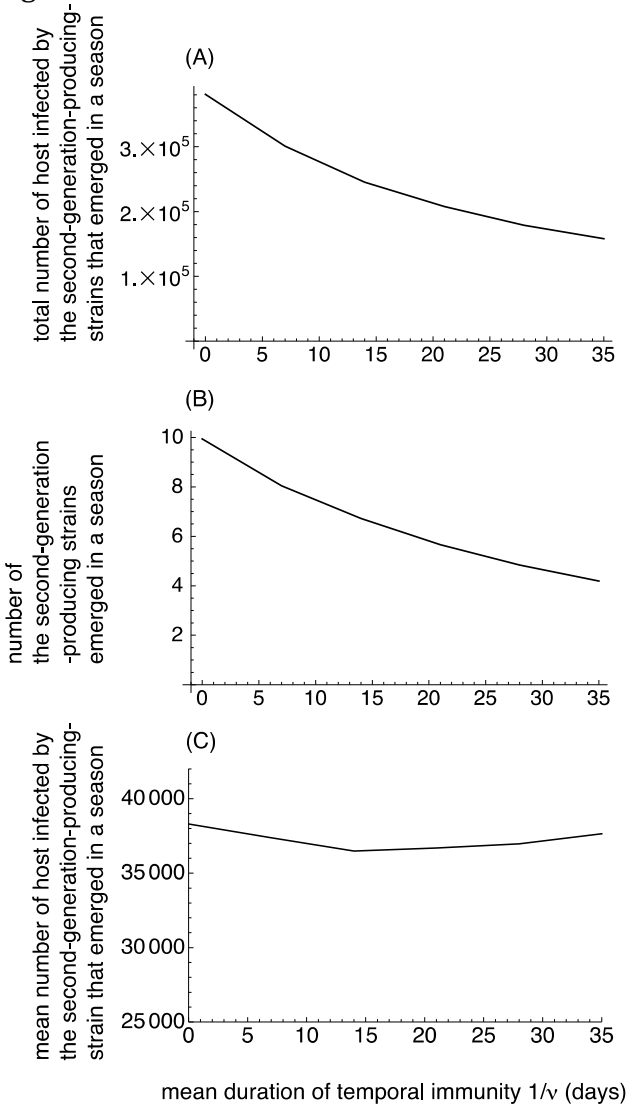
(A)
total number of host infected by the second-generation-producing-strains that emerged in a season
3.×10^5
2.×10^5
1.×10^5
0 5 10 15 20 25 30 35
(B)
number of the second-generation -producing strains emerged in a season
10
8
6
4
2
0 5 10 15 20 25 30 35
(C)
mean number of host infected by the second-generation-producing-strain that emerged in a season
40 000
35 000
30 000
25 000
0 5 10 15 20 25 30 35
mean duration of temporal immunity 1/ν (days)

fig A8

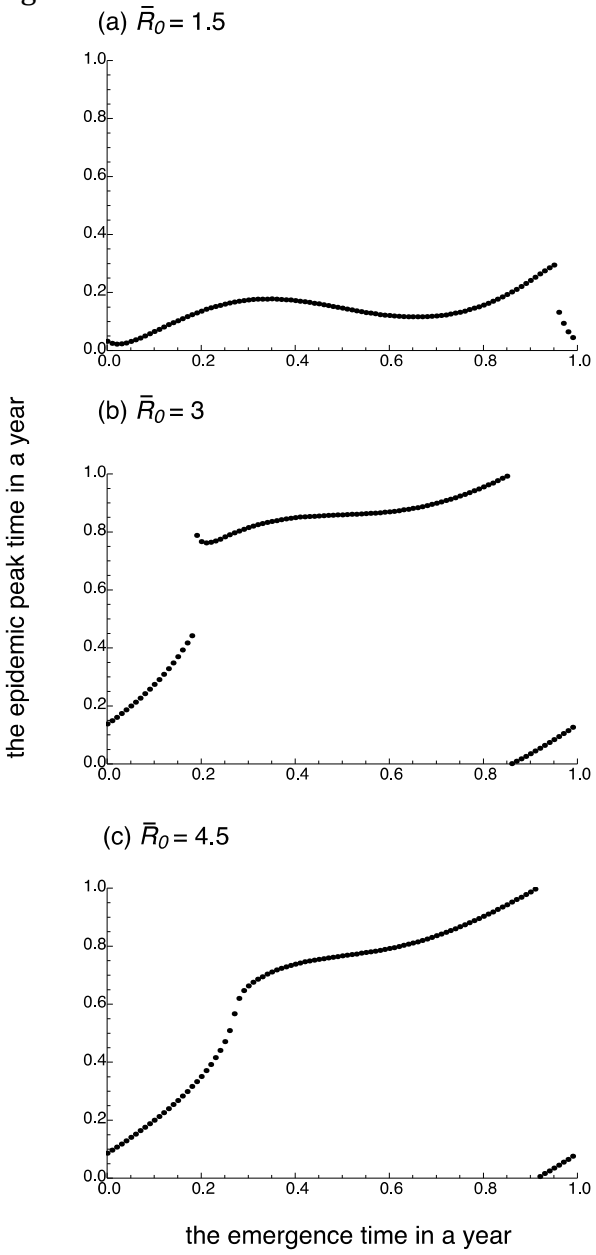
(a) $\bar{R}_0 = 1.5$
(b) $\bar{R}_0 = 3$
(c) $\bar{R}_0 = 4.5$
the epidemic peak time in a year
the emergence time in a year
0.0
0.2
0.4
0.6
0.8
1.0